Reversible molecular pathology of skeletal muscle in spinal muscular atrophy

HMG Advance Access published August 12, 2011

Reversible molecular pathology of skeletal muscle in spinal muscular atrophy

Chantal A. Mutsaers[1,2]†, Thomas M. Wishart[1,2]†, Douglas J. Lamont[3], Markus Riessland[4], Julia Schreml[4], Laura H. Comley[1,2], Lyndsay M. Murray[1,2], Simon H. Parson[1,2], Hanns Lochmüller[5], Brunhilde Wirth[4], Kevin Talbot[6] & Thomas H. Gillingwater[1,2]*

[1] Euan MacDonald Centre for Motor Neurone Disease Research & [2] Centre for Integrative Physiology, University of Edinburgh, Edinburgh, UK
[3] 'FingerPrints' Proteomics Facility, College of Life Sciences, University of Dundee, Dundee, UK
[4] Institute of Human Genetics, Institute for Genetics and Center for Molecular Medicine Cologne, University of Cologne, Cologne 50931, Germany
[5] Institute of Genetic Medicine, University of Newcastle, Newcastle Upon Tyne, UK
[6] Nuffield Department of Clinical Neurosciences, University of Oxford, Oxford, UK

† These authors contributed equally to this study

* Corresponding Author:

Thomas H. Gillingwater

Euan MacDonald Centre for Motor Neurone Disease Research & Centre for Integrative Physiology

University of Edinburgh

Edinburgh

EH8 9XD

UK

Email: T.Gillingwater@ed.ac.uk

Tel: +44 (0)131 6503724

Fax : +44 (0)131 6504193

ABSTRACT

Low levels of full-length Survival Motor Neuron (SMN) protein cause the motor neuron disease Spinal Muscular Atrophy (SMA). Whilst motor neurons undoubtedly contribute directly to SMA pathogenesis, the role of muscle is less clear. We demonstrate significant disruption to the molecular composition of skeletal muscle in pre-symptomatic severe SMA mice, in the absence of any detectable degenerative changes in lower motor neurons and with a molecular profile distinct from that of denervated muscle. Functional cluster analysis of proteomics data and phospho-histone H2AX labelling of DNA damage revealed increased activity of cell death pathways in SMA muscle. Robust up-regulation of Vdac2 and down-regulation of parvalbumin in severe SMA mice was confirmed in a milder SMA mouse model and in human patient muscle biopsies. Molecular pathology of skeletal muscle was ameliorated in mice treated with the FDA-approved histone deacetylase inhibitor, SAHA. We conclude that intrinsic pathology of skeletal muscle is an important and reversible event in SMA and also suggest that muscle proteins have the potential to act as novel biomarkers in SMA.

INTRODUCTION

Proximal autosomal spinal muscular atrophy (SMA) is a predominantly childhood form of motor neuron disease and is the most common genetic cause of infant mortality, with an incidence of 1:6,000-10,000 and a carrier frequency of 1:35 [1,2]. SMA is caused by low expression levels of full-length survival motor neuron (SMN) protein, resulting from disruption of the survival motor neuron (*SMN1*) gene [3,4]. There are two nearly identical copies of this gene in humans; the telomeric *SMN1* gene and the centromeric *SMN2* gene. The *SMN2* gene, however, produces only 10% of full length SMN protein due to a defective splicing pattern [4,5]. Retention of at least one copy of *SMN2* in SMA patients therefore leads to low residual levels of SMN protein. Although SMN protein is ubiquitously expressed, the major pathological hallmarks of SMA are focussed on the neuromuscular system, including a loss of lower motor neurons from the ventral horn of the spinal cord and atrophy of skeletal muscle [6-9].

Whilst most research to date has focussed on examining how low levels of SMN lead to pathological changes in motor neurons, the contribution of muscle to the pathogenesis of SMA remains unclear. Although pathological changes in SMA muscle, including evidence of increased levels of apoptosis, are a well-established hallmark of SMA [10-14], it has generally been assumed that changes in muscle occur simply as a secondary consequence of the degeneration of innervating lower motor neurons, rendering muscle fibres denervated. Studies have shown that restoring SMN protein levels in neurons can significantly ameliorate disease progression in SMA animal models [15,16]. However, these studies could not rule out an additional contribution resulting from restoration of SMN levels in muscle, raising the possibility that intrinsic responses to low levels of SMN in skeletal muscle may also contribute directly to SMA pathogenesis [15,17-24]. Moreover, SMN protein is present in

muscle sarcomeres from both mice and *Drosophila*, alongside other associated SMN complex proteins such as gemins [22,25]. Establishing whether skeletal muscle directly contributes to SMA pathogenesis therefore remains a critical question for understanding SMA pathogenesis as well as for the successful targeting of future therapeutic strategies. Previous attempts to address this question have been hampered, at least in part, by the fact that it has proven difficult to distinguish secondary pathological changes, induced as a consequence of denervation due to functional and structural deficits in lower motor neurons, from changes intrinsic to muscle. Moreover, studies of isolated muscle fibres from human SMA patients *in vitro* [20,24,26] are similarly defined by the fact that they are, as a direct result of the experimental protocol, devoid of lower motor neuron innervation and therefore denervated.

Here, we have utilised a skeletal muscle preparation from an established mouse model of severe SMA (*Smn*$^{-/-}$;*SMN2*$^{+/+}$) [27] where it is possible to examine molecular changes occurring in skeletal muscle *in vivo*, in the absence of any detectable denervation-inducing changes in corresponding lower motor neurons. We used this preparation to reveal modifications in the molecular composition of skeletal muscle in SMA mice at a pre-symptomatic age, with a molecular profile distinct from that of denervated muscle. Our findings were confirmed in a milder mouse model of SMA and also in muscle biopsies from human SMA patients. Finally, we demonstrate molecular pathology of skeletal muscle in SMA mice can be ameliorated by treatment with the FDA-approved histone deacetylase inhibitor, SAHA.

RESULTS

The rostral band of levator auris longus allows examination of intrinsic changes to skeletal muscle in SMA

In order to isolate and identify molecular changes occurring specifically in skeletal muscle during SMA, it is necessary to have an experimental system where low levels of SMN protein are present in muscle, but denervation due to degeneration of innervating lower motor neurons is absent. The homogeneous fast-twitch *levator auris longus* (LAL) muscle has two distinct bands (rostral and caudal) [28]. Motor neurons innervating the caudal band in the *Smn*$^{-/-}$*;SMN2* mouse model of severe SMA [27] are susceptible to SMA pathology (even at late-symptomatic stages), whereas those innervating the rostral band are resistant (see Fig 1A) [28-30]. Importantly, our group and others have previously demonstrated that motor neurons innervating the rostral LAL develop normally in the pre-symptomatic period [30], with genetic and electrophysiological studies similarly indicating an absence of lower motor neuron pathology or neuromuscular junction dysfunction in the rostral LAL from early-symptomatic SMA mice [31,32].

We validated the absence of any degenerative pathology in lower motor neurons innervating the rostral LAL in *Smn*$^{-/-}$*;SMN2* mice at a pre-symptomatic age (postnatal day 1; P1; Fig 1B): >98% of neuromuscular junctions were fully innervated by intact motor axon collaterals in both *Smn*$^{-/-}$*;SMN2* mice and littermate controls and there was no evidence of abnormal neurofilament accumulations in motor nerve terminals in any of the muscles examined (N>5 mice per genotype). Similarly, we found no evidence for denervation-induced muscle fibre shrinkage in the rostral LAL from *Smn*$^{-/-}$*;SMN2* mice at P1 (Fig 1C). Taken together with the previously published studies, we concluded that the rostral LAL at P1 represents a muscle preparation from an SMA mouse where no detectable neuronal degeneration or muscle

denervation is present, making it ideal for intrinsic molecular studies of muscle in SMA. As expected, however, there was still a 70-80% reduction in expression levels of SMN protein in the rostral LAL from *Smn*$^{-/-}$*;SMN2* mice at P1 compared with control littermates (Fig 1D).

Label-free proteomics analysis of rostral LAL reveals molecular alterations to skeletal muscle in pre-symptomatic Smn$^{-/-}$*;SMN2 mice*

Label-free proteomics techniques were used to quantify and compare the molecular composition of the rostral LAL from P1 *Smn*$^{-/-}$*;SMN2* mice compared to littermate controls (*Smn*$^{+/+}$*;SMN2*; N=9 mice per genotype; see methods). Direct comparison of rostral LAL proteomes revealed that 65 out of the 345 identified individual proteins (19%) were up-regulated >20% in *Smn*$^{-/-}$*;SMN2* mice (Table I & Supplementary Table I). Of these, 20 proteins showed a greater than 2-fold increase in expression levels. In addition, 32 out of the 345 identified proteins (9%) were down-regulated >20% in *Smn*$^{-/-}$*;SMN2* mice (Table II & Supplementary Table II). The increased expression profiles of many proteins in *Smn*$^{-/-}$*;SMN2* tissue confirmed that the changes observed were active responses to low levels of SMN in muscle, and were not simply occurring as a result of a global decrease in protein synthesis. We initially validated the proteomics data by quantifying expression levels of one significantly downregulated protein (parvalbumin) in immunohistochemically labelled muscle preparations (Supplementary Fig 1).

To identify any functional clustering of proteins found to have modified expression levels in the rostral LAL of SMA mice, we performed a systems level analysis of the proteomics data using Ingenuity Pathway Analysis software. 83 out of the 97 proteins identified were listed in this software and therefore available for data mining of the existing published literature to determine potential functional clustering. This analysis revealed that many of the proteins

with modified expression profiles in muscle from *Smn*$^{-/-}$*;SMN2* mice are reported to regulate muscle function and pathology (Table III). For example, the functional cluster most significantly changed in SMA muscle contained proteins known to contribute to skeletal and muscular disorders: 44 of the proteins changed in *Smn*$^{-/-}$*;SMN2* muscle (53% of the total list) have links to these disorders, 6 of which also directly contribute to myopathies (Table III). Similarly, modifications were observed in clusters of proteins contributing to cell death pathways and morphological development (Table III). A different analysis at the systems level also highlighted disruption of two protein interaction networks (identified by known direct or indirect interactions between individual proteins) implicated in development and function of the skeletal and muscular systems (Supplementary Fig 2).

Evidenced for increased cell death in SMA muscle

The finding that 35% of the proteins submitted for functional clustering analysis contribute to cell death pathways (Table III) was of particular interest given that apoptotic cell death has previously been reported in SMA muscle [10-14]. Indeed, several of the protein expression changes identified in the rostral LAL of SMA mice have previously been implicated in activation of apoptotic and non-apoptotic cell death pathways (e.g. Vdac2) [33,34]. We therefore asked whether markers of cell death were increased in the rostral LAL of *Smn*$^{-/-}$*;SMN2* mice. Immunohistochemical labelling for phospho-histone H2AX (H2AX) was used as a sensitive marker of DNA damage during the early stages of apoptosis [35,36]. Cells strongly expressing H2AX were rarely observed in rostral LAL from littermate control mice, but were readily identifiable in *Smn*$^{-/-}$*;SMN2* mice (Fig 2), suggesting a significant elevation in levels of cell death in the SMA mice. Thus, at least some of the protein expression changes identified in the rostral LAL of SMA mice (e.g. cell death proteins; see Table III) were

contributing directly to biological pathways regulating muscle responses to low SMN levels *in vivo*.

Changes in the molecular composition of skeletal muscle in SMA mice are distinct from those elicited following acute or chronic denervation

To confirm that the molecular changes observed in SMA muscle were not occurring as a result of acute or chronic denervation subsequent to motor neuron pathology, we compared our proteomics data to similar data from proteomics studies of chronically denervated muscle (>1 week following nerve injury; Fig 3A). The profile of expression changes observed in rostral LAL from SMA mice was clearly distinct from those modified following denervation (Fig 3A) [37-39]. As these previous studies were all performed on chronically denervated muscle, we also quantified expression levels of two proteins significantly altered in SMA muscle (Vdac2 and parvalbumin) in acutely denervated muscles. We lesioned the sciatic nerve in wild-type mice and isolated the denervated flexor digitorum brevis (FDB) and deep lumbrical muscles from the hind-foot 24 hours later. As expected, morphological evaluation of neuromuscular junctions confirmed complete denervation in all muscles examined (data not shown). However, levels of both Vdac2 and parvalbumin remained unchanged (Fig 3B).

Molecular pathology of muscle is also present in human SMA patients

We next examined whether molecular changes observed in pre-symptomatic SMA mice were also present in skeletal muscle from human SMA patients. Quantitative fluorescent western blotting was performed on human SMA patient *Quadriceps femoris* muscle biopsy samples, to establish expression levels of Vdac2 and parvalbumin (Fig 4). Biopsies were obtained from type II/III SMA patients (aged between 3 and 25 years old; see methods), with genetic diagnosis of SMA confirmed by a homozygous deletion of the *SMN1* gene. Three age-

matched control samples, genetically confirmed to have no mutations in the *SMN1* gene, were used for comparison. As expected, SMN protein expression levels were significantly decreased in SMA patient samples compared to control samples (Fig 4A/B). Quantitative western blotting revealed that both Vdac2 and parvalbumin showed similar alterations in expression levels to those previously observed in *Smn*$^{-/-}$*;SMN2* mice: Vdac2 was significantly up-regulated >3 fold in SMA patient muscle (Fig 4C) and parvalbumin was significantly down-regulated >4 fold (Fig 4D).

Molecular pathology of skeletal muscle is reversed by treatment with the FDA-approved histone deacetylase inhibitor, SAHA

The finding that levels of full-length SMN protein produced by the *SMN2* gene can be modulated by small molecules and drugs has raised the possibility of a therapy for SMA. For example, epigenetic modulation using histone deacetylase inhibitors (HDACi) appears to be successful [40], with the HDACi SAHA (also known as Vorinostat or Zolinza) elevating full-length SMN protein levels in SMA mouse models *in vivo*, resulting in a 30% increase in mean survival and amelioration of muscle fibre size shrinkage [41]. To examine whether HDAC inhibitors are capable of directly targeting molecular changes in muscle during SMA, we examined expression levels of Vdac2, parvalbumin and the cell death marker H2AX in skeletal muscle from SMA mice treated with SAHA.

For these experiments we used a milder SMA mouse model (Taiwanese-SMA mice) with a new breeding protocol (*Smn*$^{-/-}$*;SMN2*$^{tg/tg}$ x *Smn*$^{-/+}$) [41] to generate affected SMA mice that survive ~10 days postnatal on a congenic FVB/N genetic background. The slightly longer life-span of this model is better for testing potential therapeutic agents than the more severe *Smn*$^{-/-}$*;SMN2* model [41]. We first confirmed that molecular pathological changes similar to

those observed in *Smn*$^{-/-}$*;SMN2* mice were also present in untreated late-symptomatic (P10) Taiwanese-SMA mice. As expected, SMN protein levels in the *gastrocnemius* muscle were reduced to around 25% of those in littermate controls (Fig 5A/B). Vdac2 levels were increased (Fig 5C) and parvalbumin levels were decreased (Fig 5D) in Taiwanese-SMA mice, and increased cell death was confirmed by an increase in levels of H2AX (Fig 5E). Importantly, it has previously been demonstrated that neuronal pathology is present in the *gastrocnemius* muscle of Taiwanese-SMA mice at P10 (including denervation of muscle fibres) [41]. Thus, the molecular changes initially observed in the LAL muscle of severe SMA mice at P1 in the absence of neuronal pathology were also present in anatomically distinct muscles susceptible to denervation in SMA.

Taiwanese-SMA mice and littermate controls were treated with SAHA from birth via oral administration of 25mg/kg SAHA (dissolved in DMSO) twice daily [41]. For control experiments, mice were dosed with DMSO alone. As previously reported [41], SAHA treatment significantly increased SMN protein expression levels in the *gastrocnemius* muscle (Fig 5). Importantly, however, SAHA treatment significantly ameliorated SMN-induced changes in levels of Vdac2, parvalbumin and H2AX (Fig 5).

DISCUSSION

In this study we have identified and characterised molecular pathology of skeletal muscle in an established mouse model of severe SMA. These changes were present during the earliest stages of disease and occured in the absence of any detectable degeneration of lower motor neurons. The molecular profile of muscle pathology in SMA was distinct from that of denervated muscle, with functional cluster analysis of proteomics data and H2AX labelling highlighting increased activity of cell death pathways. We confirmed the robust up-regulation of Vdac2 and down-regulation of parvalbumin in a different (milder) SMA mouse model and also in human patient muscle biopsies. Molecular pathology of skeletal muscle was ameliorated in mice treated with the FDA-approved HDACi SAHA.

This study provides significant *in vivo* experimental data from mouse models and human patient material to support the hypothesis that SMA-induced changes in muscle cannot solely be attributed to motor neuron degeneration. For example, the molecular changes we identified in SMA muscle were distinct from those reported in chronically or acutely denervated muscle. The proposal that muscle changes can occur in the absence of neuronal pathology in SMA is supported by several previous studies. For example, studies of SMN protein expression and localisation have identified the SMN complex in muscle from both mice and *Drosophila*, as well as in C2C12 cells *in vitro* [21,22,25]. Moreover, *in vitro* studies have shown that muscle cells derived from SMA patients can inhibit neuronal outgrowth and development when co-cultured with wild-type healthy motor neurons [12,17,42] and a recent study of myotubes from human SMA fetuses also revealed a delay in growth and maturation *in vitro* [24]. Moreover, fibroblast growth factor (FGF) signalling in muscle can ameliorate SMN-associated abnormalities at the neuromuscular junction in *Drosophila* [43] and increased levels of insulin-like growth factor (IGF-1) in muscle modulates SMA phenotype in

mice [44]. Taken together, these findings suggest SMN levels are critical for the establishment and maintenance of molecular homeostasis in skeletal muscle. Thus, direct disruption of muscle resulting from low levels of SMN is likely to be a significant contributor to SMA pathogenesis, alongside pathological changes in motor neurons.

Interestingly, many of the proteins shown to have altered expression profiles in skeletal muscle during SMA have previously been implicated in other neuromuscular diseases where intrinsic muscle pathology occurs. For example, decorin is associated with modified proliferation and differentiation of myogenic cells in x-linked muscular dystrophy [45] and reticulocalbin 1 expression is altered in dystrophic muscles [46]. Galectin 1 has been implicated in myoblast differentiation, skeletal muscle development and muscle regeneration [47,48]. Similarly, proteins such as serpin H1 (a.k.a. HSP47) and vinculin, through its interaction with dysferlin, have been implicated in muscle fibre repair and maintenance of the muscle membrane respectively [49,50]. Thus, the proteins we identified as have altered expression profiles in SMA muscle are consistent with those that might be expected to regulate intrinsic muscular pathology based on findings from other neuromuscular disorders.

Two proteins of particular interest in the context of this study are Vdac2 and parvalbumin. Both showed modified expression levels in skeletal muscle across two different mouse models of SMA as well as in human patients, and both responded significantly to SAHA treatment. This raises the possibility of their use as novel biomarkers to report directly on the pathological status of the neuromuscular system in human patients. Such biomarkers are urgently required for clinical trials in SMA patient cohorts, where appropriate molecular biomarkers are currently lacking. The observation that the expression profiles of these two proteins are changed in opposing directions in SMA further strengthens their potential utility

as biomarkers, providing an internal control against any global up- or down-regulation of protein expression in individual patients. Vdac2 is a mitochondrial protein associated with formation of channels in the mitochondrial outer membrane, responsible for regulating cell death pathways and calcium signalling [51-53]. It is also a core component of the muscle response to aging [54] and has been implicated in early pathogenic events occurring in the mdx mouse model of muscular dystrophy [55]. Parvalbumin is a cytosolic calcium buffer in muscle, breakdown of which similarly contributes to muscular dystrophy [56,57].

Finally, our finding that the altered molecular composition of skeletal muscle in SMA is reversible using the HDACi SAHA highlights the potential to treat SMN-induced muscle changes using small molecules and drugs. SAHA has been shown to penetrate into a range of tissues following administration - including the nervous system and muscle [41,58,59] - and is approved for use in humans by the FDA in the US. SAHA is a second generation HDACi, so it is likely that future generations will have even higher specificity and potency, increasing their attractiveness for use in SMA patients. Our findings suggest that attempts to develop better HDACi that specifically target SMN levels in skeletal muscle would likely lead to effective therapeutic options for SMA. Testing other currently available HDACi for the potential to rescue muscle pathology *in vivo* will also be an important next step. The current data do not allow us to ascertain whether raised SMN levels in muscle induced by SAHA also have a secondary impact on pathological changes occurring in other cell types (e.g. motor neurons), due to systemic delivery of the HDACi [41]. Thus, the potential for a causal relationship between the rescue of pathological changes occurring in muscle in SAHA treated SMA mice and the reduction in pathology of motor neurons previously reported [41] remains untested and warrants further investigation. Nevertheless, the current study shows that

intrinsic pathological changes in muscle are a significant feature of SMA, regardless of their possible secondary impact on other cell types.

MATERIALS AND METHODS

Mice

Smn$^{+/-}$*;SMN2* mice (Jackson labs strain no. 005024) were maintained as heterozygote breeding pairs under standard SPF conditions in animal care facilities in Edinburgh. Litters produced from SMA colonies were retrospectively genotyped using standard PCR protocols (JAX® Mice Resources), as previously described [29]. Taiwanese-SMA mice were bred and maintained in micro-isolation chambers in Cologne as previously reported [41]. For SAHA experiments, litters of Taiwanese-SMA mice (containing SMA mice and littermate controls) were dosed twice daily from birth with either 25mg/kg SAHA dissolved in DMSO, or an equivalent volume of DMSO alone, via oral application with a feeding needle. All animal procedures and breeding were performed in accordance with Home Office guidelines in the UK and according to guidelines established by the Landesamt fur Natur, Umwelt und Verbraucherschutz NRW in Germany.

Human Muscle Samples

Quadriceps femoris biopsy samples were obtained from Fondazione IRCCS Istituto Neurologico “C. Besta” in Milan, Italy and Fondazione Ospedale Maggiore Polclinico Mangiagalli en Regina Elena, IRCCS in Milan, Italy through EuroBioBank (http://www.eurobiobank.org/).

Acute Nerve Degeneration

Young adult wild-type (C57Bl/6J) mice (n=4) were anaesthetized by inhalation of isofluorane (2%, 1:1 N_2O/O_2) before exposing the sciatic nerve in the thigh and removing 1mm section of the nerve to ensure complete transection. Post-operative mice were kept in standard animal house conditions for 24 hours before sacrifice.

Muscle Preparation

Mouse: neonatal *Smn*$^{-/-}$*;SMN2* and wild-type (*Smn*$^{+/+}$*;SMN2*) littermates were sacrificed by chilling on ice and decapitation. *Levator auris longus* (LAL, from the back of the neck) [28] muscles were dissected in oxygenated mammalian physiological saline. For proteomics and quantitative western blotting experiments, LAL muscles were separated into rostral and caudal bands and quickly frozen on dry ice. The muscles were stored in -80^{o}C freezers until enough tissue was collected for analysis. C56Bl6/J mice subjected to sciatic nerve lesion were sacrificed and the *flexor digitorum brevis* (FDB) and deep lumbrical muscles were isolated. Muscle were either processed for immunohistochemistry or rapidly frozen on dry ice for subsequent western blotting. Neonatal Taiwanese-SMA mice and littermate controls were sacrificed and the *gastrocnemius* muscles dissected and immediately flash-frozen before storing at -80^{o}C before being shipped to Edinburgh for analysis.

Human: human tissues in the form of muscle biopsies were obtained from two different biobanks. Proteins from muscle biopsies were extracted in RIPA buffer with 10% protease inhibitor cocktail (Sigma) for quantitative western blotting.

Label-free proteomics

Protein was extracted in MEBC Buffer (50 mM TRIS, 100 mM NaCl, 5 mM NaEDTA, 5 mM NaEGTA, 40 mM β-glycerophosphate, 100 mM sodium fluoride (NaF), 100 mM

sodium orthovanadate, 0.25% NP-40, 1 Roche 'complete' protease inhibitor tablet, pH 7.4). Protein concentration was determined by BCA assay according to manufacturers instructions on solubilised muscle (WT-Rostral and KO-Rostral). Then 10ug aliquots of each muscle type were reduced with 10 mM DTT and alkylated with 50 mM iodoacetamide prior to digestion with trypsin (Roche, sequencing grade) overnight at 30oC. Technical replicates (3 x 2.5 ug) of each digested muscle type were injected onto a nLC-MS/MS system (Ultimate 3000 (Dionex) coupled to a LTQ Orbitrap XL (Thermo Scientific). The peptides from each digest were separated over a 65 min linear gradient from 5-35% acetonitrile in 0.1% formic acid. The LTQ Orbitrap XL was configured with a TOP 5 methodology comprising a 60K resolution FT-MS full scan followed by IT-MS/MS scans for the 5 most intense peptide ions. The raw data was then imported into Progenesis LCMS for label free differential analysis and subsequent identification and quantitation of relative ion abundance ratios, both up-regulated and down-regulated. Individual peptide sequences generated by the proteomics analysis were submitted to MASCOT for protein identification. A stringent selection criteria was used before a protein was included; identification of at least two peptides was needed, a minimum cut-off of 20% change against the littermate controls was used and a p value of <0.05 [60,61].

Quantitative fluorescent western blotting

Protein was extracted from both human and mouse muscle samples. Quantitative western blots were performed as described previously [60,62], using primary antibodies against SMN (BD Transduction laboratories or Santa Cruz), VDAC-2 (Abcam), Parvalbumin (Abcam), phospho-histone H2AX (Upstate) and beta-V-Tubulin (Abcam). Odyssey secondary antibodies were added according to manufacturers instructions (Goat anti rabbit IRDye 680 or 800 and Goat anti mouse IRDye 680 or 800 dependant on required combinations). Blots were imaged using an Odyssey Infrared Imaging System (Li-COR, Biosciences) at 169µm

resolution. Where possible, each sample was independently run and measured multiple times to minimise user variability.

In silico protein network and functional pathway analysis

To obtain further insights into functional pathways modified as a result of low SMN levels in muscle, the Ingenuity Pathways Analysis (IPA) application (Ingenuity Systems) was used to analyse our proteomics data. IPA dynamically generates network of gene, protein, small molecule, drug, and disease associations on the basis of "hand-curated" data held in a proprietary database. Of the submitted protein candidate list (97 proteins in total), 83 proteins were recognized by the software and therefore eligible for pathway analysis.

NMJ Immunohistochemistry and Muscle Fibre Diameter Measurements

LALs from *Smn*$^{-/-}$*;SMN2* and littermate controls (P1 or P5) or FDB and deep lumbrical muscles from C56Bl6/J mice were fixed in 0.1M PBS containing 4% paraformaldehyde (Electron Microscopy Services) for 10 min and then exposed to α-BTX conjugated to tetramethyl-rhodamin isothiocyanate (TRITC-α-BTX; 5mg/ml, Molecular Probes) to label post-synaptic acetylcholine receptors. Muscles were then processed for immunohistochemistry as previously described [29]. Primary antibodies against either neurofilament (2H3, Developmental Studies Hybridoma Bank) or phospho-histone H2AX (Upstate) were used. Before mounting in mowoil, the dissections were incubated in TOPRO3 (Molecular probes) for 10 min. Fluorescence images were captured using a laser scanning confocal microscope (40x objective; ZEISS LSM 510) with 488nm, 543nm and 633 nm laser lines used for excitation. Confocal Z-series were merged using Zeiss software. Reconstructions of FITC-labelled muscle preparations were produced using Adobe Photoshop software by layering and combining multiple micrographs covering the entire

muscle. All images were prepared for publication using Adobe Photoshop. For muscle fibre diameter measurements, individual muscle fibre diameters were imaged using phase contrast optics on an inverted microscope equipped with a chilled CCD camera (20x/0.40 objective; Olympus IX71 microscope; Hammamatsu C4742-96-12G04) and measurements were made using ImageJ.

Statistical analysis

All data were collected into Microsoft Excel spreadsheets and then analysed using GraphPad Prism software. For all statistical analyses, $P<0.05$ was considered to be significant. Individual statistical tests used are detailed in the results section or figure legends.

ACKNOWLEDGEMENTS

The authors are grateful to members of the Gillingwater and Parson laboratories for advice and assistance with this study, Derek Thomson for help with mouse breeding, Kenneth Beattie and Dr Wenzhang Chen for assistance with proteomics experiments, and Professor Angela Vincent for helpful comments on an earlier version of the manuscript. We thank the Telethon Biobank, supported by TELETHON grants (project no GTB07001), and gratefully acknowledge the assistance of Maurizio Moggio and Monica Sciacco in providing human muscle samples.

This work was supported by grants from the SMA Trust (to THG), BDF Newlife (to THG/KT/SHP), the Anatomical Society (to THG/LM/SHP), and the Deutsche Forschungsgemeinschaft (to BW).

CONFLICT OF INTEREST STATEMENT

The authors have no conflicts of interest to declare.

REFERENCES

1. Pearn J (1978) Incidence, prevalence, and gene frequency studies of chronic childhood spinal muscular atrophy. *J. Med. Genet.,* **15,** 409-413.

2. Wirth B (2000) An update of the mutation spectrum of the survival motor neuron gene (SMN1) in autosomal recessive spinal muscular atrophy (SMA). *Hum. Mutat.,* **15,** 228-237.

3. Lefebvre S, Bürglen L, Reboullet S, Clermont O, Burlet P, Viollet L, Benichou B, Cruaud C, Millasseau P, Zeviani M, et al. (1995) Identification and characterization of a spinal muscular atrophy-determining gene. *Cell,* **80**, 155-165.

4. Burghes AH, Beattie CE (2009) Spinal muscular atrophy: why do low levels of survival motor neuron protein make motor neurons sick? *Nat. Rev. Neurosci.,* **10**, 597-609.

5. Lorson CL, Rindt H, Shababi M (2010) Spinal muscular atrophy: mechanisms and therapeutic strategies. *Hum. Mol. Genet.,* **19,** R111-118.

6. Swoboda KJ, Prior TW, Scott CB, McNaught TP, Wride MC, Reyna SP, Bromberg MB (2005) Natural history of denervation in SMA: relation to age, SMN2 copy number, and function. *Ann. Neurol.,* **57**, 704-712.

7. Lunn MR, Wang CH (2008) Spinal muscular atrophy. *Lancet,* **371**, 2120-2133.

8. Murray LM, Talbot K, Gillingwater TH (2010) Neuromuscular synaptic vulnerability in motor neurone disease: amyotrophic lateral sclerosis and spinal muscular atrophy. *Neuropathol. Appl. Neurobiol.,* **36,** 133-156.

9. Sleigh JN, Gillingwater TH, Talbot K (2011) The contribution of mouse models to understanding the pathogenesis of spinal muscular atrophy. *Dis. Model. Mech.,* **4,** 457-467.

10. Fidziańska A, Goebel HH, Warlo I (1990) Acute infantile spinal muscular atrophy. Muscle apoptosis as a proposed pathogenetic mechanism. *Brain,* **113,** 433-445.

11. Tews DS, Goebel HH (1997) Apoptosis-related proteins in skeletal muscle fibers of spinal muscular atrophy. *J. Neuropathol. Exp. Neurol.,* **56,** 150-156.

12. Guettier-Sigrist S, Hugel B, Coupin G, Freyssinet JM, Poindron P, Warter JM (2002) Possible pathogenic role of muscle cell dysfunction in motor neuron death in spinal muscular atrophy. *Muscle Nerve,* **25,** 700-708.

13. Stathas D, Kalfakis N, Kararizou E, Manta P (2008) Spinal muscular atrophy: DNA fragmentation and immaturity of muscle fibers. *Acta Histochem.,* **110,** 53-58.

14. Dachs E, Hereu M, Piedrafita L, Casanovas A, Calderó J, Esquerda JE. (2011) Defective neuromuscular junction organization and postnatal myogenesis in mice with severe spinal muscular atrophy. *J. Neuropathol. Exp. Neurol.,* **70,** 444-461.

15. Chan YB, Miguel-Aliaga I, Franks C, Thomas N, Trülzsch B, Sattelle DB, Davies KE, van den Heuvel M (2003) Neuromuscular defects in a Drosophila survival motor neuron gene mutant. *Hum. Mol. Genet.,* **12,** 1367-1376.

16. Gavrilina TO, McGovern VL, Workman E, Crawford TO, Gogliotti RG, DiDonato CJ, Monani UR, Morris GE, Burghes AH (2008) Neuronal SMN expression corrects spinal muscular atrophy in severe SMA mice while muscle-specific SMN expression has no phenotypic effect. *Hum. Mol. Genet.,* **17,** 1063-1075.

17. Braun S, Croizat B, Lagrange MC, Warter JM, Poindron P. (1995) Constitutive muscular abnormalities in culture in spinal muscular atrophy. *Lancet,* **345,** 694-695.

18. Greensmith L, Vrbová G (1997) Disturbances of neuromuscular interaction may contribute to muscle weakness in spinal muscular atrophy. *Neuromuscul. Disord.,* **7,** 369-372.

19. Cifuentes-Diaz C, Frugier T, Tiziano FD, Lacène E, Roblot N, Joshi V, Moreau MH, Melki J (2001) Deletion of murine SMN exon 7 directed to skeletal muscle leads to severe muscular dystrophy. *J. Cell Biol.,* **152,** 1107-1114.

20. Arnold AS, Gueye M, Guettier-Sigrist S, Courdier-Fruh I, Coupin G, Poindron P, Gies JP (2004) Reduced expression of nicotinic AChRs in myotubes from spinal muscular atrophy I patients. *Lab. Invest.,* **84,** 1271-1278.

21. Shafey D, Côté PD, Kothary R (2005) Hypomorphic Smn knockdown C2C12 myoblasts reveal intrinsic defects in myoblast fusion and myotube morphology. *Exp. Cell Res.,* **311,** 49-61.

22. Rajendra TK, Gonsalvez GB, Walker MP, Shpargel KB, Salz HK, Matera AG (2007) A Drosophila melanogaster model of spinal muscular atrophy reveals a function for SMN in striated muscle. *J. Cell Biol.,* **176,** 831-841.

23. Vrbova G (2008) Spinal muscular atrophy: motoneurone or muscle disease? *Neuromuscul. Disord.,* **18,** 81-82.

24. Martínez-Hernández R, Soler-Botija C, Also E, Alias L, Caselles L, Gich I, Bernal S, Tizzano EF (2009) The developmental pattern of myotubes in spinal muscular atrophy indicates prenatal delay of muscle maturation. *J. Neuropathol. Exp. Neurol.,* **68,** 474-481.

25. Walker MP, Rajendra TK, Saieva L, Fuentes JL, Pellizzoni L, Matera AG (2008) SMN complex localizes to the sarcomeric Z-disc and is a proteolytic target of calpain. *Hum. Mol. Genet.,* **17,** 3399-3410.

26. Anderson K, Potter A, Baban D, Davies KE (2003) Protein expression changes in spinal muscular atrophy revealed with a novel antibody array technology. *Brain,* **126,** 2052-2064.

27. Monani UR, Sendtner M, Coovert DD, Parsons DW, Andreassi C, Le TT, Jablonka S, Schrank B, Rossoll W, Prior TW, et al. (2000) The human centromeric survival motor neuron

gene (SMN2) rescues embryonic lethality in Smn(-/-) mice and results in a mouse with spinal muscular atrophy. *Hum. Mol. Genet.,* **9**, 333-339.

28. Murray LM, TH Gillingwater, Parson SH (2010) Using mouse cranial muscles to investigate neuromuscular pathology in vivo. *Neuromuscul. Disord.,* **20,** 740-743.

29. Murray LM, Comley LH, Thomson D, Parkinson N, Talbot K, Gillingwater TH (2008) Selective vulnerability of motor neurons and dissociation of pre- and post-synaptic pathology at the neuromuscular junction in mouse models of spinal muscular atrophy. *Hum. Mol. Genet.,* **17,** 949-962.

30. Murray LM, Sheena L, Bäumer D, Parson SH, Talbot K, Gillingwater TH (2010) Pre-symptomatic development of lower motor neuron connectivity in a mouse model of severe spinal muscular atrophy. *Hum. Mol. Genet.,* **19,** 420-433.

31. Bäumer D, Lee S, Nicholson G, Davies JL, Parkinson NJ, Murray LM, Gillingwater TH, Ansorge O, Davies KE, Talbot K (2009) Alternative splicing events are a late feature of pathology in a mouse model of spinal muscular atrophy. *PLoS Genet.,* **5**, e1000773.

32. Ruiz R, Casañas JJ, Torres-Benito L, Cano R, Tabares L (2010) Altered intracellular Ca2+ homeostasis in nerve terminals of severe spinal muscular atrophy mice. *J. Neurosci.,* **30,** 849-857.

33. Yagoda N, von Rechenberg M, Zaganjor E, Bauer AJ, Yang WS, Fridman DJ, Wolpaw AJ, Smukste I, Peltier JM, Boniface JJ, et al. (2007) RAS-RAF-MEK-dependent oxidative cell death involving voltage-dependent anion channels. *Nature,* **447,** 864-868.

34. Yamagata H, Shimizu S, Nishida Y, Watanabe Y, Craigen WJ, Tsujimoto Y (2009) Requirement of voltage-dependent anion channel 2 for pro-apoptotic activity of Bax. *Oncogene,* **28,** 3563-3572.

35. Plesca D, Mazumder S, Almasan A (2008) DNA damage response and apoptosis. *Methods Enzymol.,* **446,** 107-122.

36. Wen W, Zhu F, Zhang J, Keum YS, Zykova T, Yao K, Peng C, Zheng D, Cho YY, Ma WY, et al. (2010) MST1 promotes apoptosis through phosphorylation of histone H2AX. *J. Biol. Chem.,* **285,** 39108-39116.

37. Li Z, Lehar M, Samlan R, Flint P (2005) Proteomic analysis of rat laryngeal muscle following denervation. *Proteomics,* **5.** 4764-4776.

38. Sun H, Liu J, Ding F, Wang X, Liu M, Gu X (2006) Investigation of differentially expressed proteins in rat gastrocnemius muscle during denervation-reinnervation. *J. Muscle Res. Cell Motil.,* **27,** 241-250.

39. Sato Y, Shimizu M, Mizunoya W, Wariishi H, Tatsumi R, Buchman V, Ikeuchi Y (2009) Differential expression of sarcoplasmic and myofibrillar proteins of rat soleus muscle during denervation atrophy. *Biosci. Biotechnol. Biochem.,* **73,** 1748-1756.

40. Wirth B, Brichta L, Hahnen E (2006) Spinal muscular atrophy and therapeutic prospects. *Prog. Mol. Subcell. Biol.,* **44,** 109-132.

41. Riessland M, Ackermann B, Förster A, Jakubik M, Hauke J, Garbes L, Fritzsche I, Mende Y, Blumcke I, Hahnen E, et al. (2010) SAHA ameliorates the SMA phenotype in two mouse models for spinal muscular atrophy. *Hum. Mol. Genet.,* **19,** 1492-1506.

42. Henderson CE, Hauser SL, Huchet M, Dessi F, Hentati F, Taguchi T, Changeux JP, Fardeau M (1987) Extracts of muscle biopsies from patients with spinal muscular atrophies inhibit neurite outgrowth from spinal neurons. *Neurology,* **37,** 1361-1364.

43. Sen A, Yokokura T, Kankel MW, Dimlich DN, Manent J, Sanyal S, Artavanis-Tsakonas S (2011) Modeling spinal muscular atrophy in Drosophila links Smn to FGF signaling. *J. Cell Biol.,* **192,** 481-495.

44. Bosch-Marcé M, Wee CD, Martinez TL, Lipkes CE, Choe DW, Kong L, Van Meerbeke JP, Musarò A, Sumner CJ (2011) Increased IGF-1 in muscle modulates the phenotype of severe SMA mice. *Hum. Mol. Genet.,* **20,** 1844-1853.

45. Abe S, Hirose D, Kado S, Iwanuma O, Saka H, Yanagisawa N, Ide Y (2009) Increased expression of decorin during the regeneration stage of mdx mouse. *Anat. Sci. Int.,* **84,** 305-311.

46. Zhang Y, Ye J, Chen D, Zhao X, Xiao X, Tai S, Yang W, Zhu D (2006) Differential expression profiling between the relative normal and dystrophic muscle tissues from the same LGMD patient. *J. Transl. Med.,* **4,** 53.

47. Svensson A, Tågerud S (2009) Galectin-1 expression in innervated and denervated skeletal muscle. *Cell. Mol. Biol. Lett.,* **14,** 128-138.

48. Grossi A, Lametsch R, Karlsson AH, Lawson MA (2011) Mechanical stimuli on C2C12 myoblasts affect myoblast differentiation, focal adhesion kinase phosphorylation and galectin-1 expression: a proteomic approach. *Cell Biol. Int.,* **35,** 579-586.

49. Higuchi I, Hashiguchi A, Matsuura E, Higashi K, Shiraishi T, Hirata N, Arimura K, Osame M (2007) Different pattern of HSP47 expression in skeletal muscle of patients with neuromuscular diseases. *Neuromuscul. Disord.,* **17,** 221-226.

50. de Morrée A, Hensbergen PJ, van Haagen HH, Dragan I, Deelder AM, 't Hoen PA, Frants RR, van der Maarel SM (2010) Proteomic analysis of the dysferlin protein complex unveils its importance for sarcolemmal maintenance and integrity. *PLoS One,* **5,** e13854.

51. Cheng EH, Sheiko TV, Fisher JK, Craigen WJ, Korsmeyer SJ (2003) VDAC2 inhibits BAK activation and mitochondrial apoptosis. *Science,* **301,** 513-517.

52. Roy SS, Ehrlich AM, Craigen WJ, Hajnóczky G (2009) VDAC2 is required for truncated BID-induced mitochondrial apoptosis by recruiting BAK to the mitochondria. *EMBO Rep.,* **10,** 1341-1347.

53. Subedi KP, Kim JC, Kang M, Son MJ, Kim YS, Woo SH (2011) Voltage-dependent anion channel 2 modulates resting Ca^{2+} sparks, but not action potential-induced Ca^{2+} signaling in cardiac myocytes. *Cell Calcium,* **49,** 136-143.

54. O'Connell K, Ohlendieck K (2009) Proteomic DIGE analysis of the mitochondria-enriched fraction from aged rat skeletal muscle. *Proteomics,* **9,** 5509-5524.

55. Massa R, Marliera LN, Martorana A, Cicconi S, Pierucci D, Giacomini P, De Pinto V, Castellani L (2000) Intracellular localization and isoform expression of the voltage-dependent anion channel (VDAC) in normal and dystrophic skeletal muscle. *J. Muscle Res. Cell. Motil.,* **21,** 433-442.

56. Gailly P (2002) New aspects of calcium signaling in skeletal muscle cells: implications in Duchenne muscular dystrophy. *Biochim. Biophys. Acta.,* **1600,** 38-44.

57. Rome LC (2006) Design and function of superfast muscles: new insights into the physiology of skeletal muscle. *Annu. Rev. Physiol.,* **68,** 193-221.

58. Hockly E, Richon VM, Woodman B, Smith DL, Zhou X, Rosa E, Sathasivam K, Ghazi-Noori S, Mahal A, Lowden PA, et al. (2003) Suberoylanilide hydroxamic acid, a histone deacetylase inhibitor, ameliorates motor deficits in a mouse model of Huntington's disease. *Proc. Natl. Acad. Sci. U.S.A.,* **100,** 2041-2046.

59. Hahnen E, Eyüpoglu IY, Brichta L, Haastert K, Tränkle C, Siebzehnrübl FA, Riessland M, Hölker I, Claus P, Romstöck J, et al. (2006) In vitro and ex vivo evaluation of second-generation histone deacetylase inhibitors for the treatment of spinal muscular atrophy. *J. Neurochem.,* **98,** 193-202.

60. Wishart TM, Huang JP, Murray LM, Lamont DJ, Mutsaers CA, Ross J, Geldsetzer P, Ansorge O, Talbot K, Parson SH, et al. (2010) SMN deficiency disrupts brain development in a mouse model of severe spinal muscular atrophy. *Hum. Mol. Genet.,* **19,** 4216-4228.

61. Comley LH, Fuller HR, Wishart TM, Mutsaers CA, Thomson D, Wright AK, Ribchester RR, Morris GE, Parson SH, Horsburgh K, et al. (2011) ApoE isoform-specific regulation of regeneration in the peripheral nervous system. *Hum. Mol. Genet.,* **20,** 2406-2421.

62. Wishart TM, Paterson JM, Short DM, Meredith S, Robertson KA, Sutherland C, Cousin MA, Dutia MB, Gillingwater TH (2007) Differential proteomics analysis of synaptic proteins identifies potential cellular targets and protein mediators of synaptic neuroprotection conferred by the slow Wallerian degeneration (Wlds) gene. *Mol. Cell. Proteomics,* **6,** 1318-1330.

LEGENDS TO FIGURES

Figure 1. The rostral band of the LAL in pre-symptomatic SMA mice provides an experimental model to study SMN-induced changes in the molecular composition of muscle in the absence of neuronal pathology. (A) The middle panel shows a low-magnification overview of the entire muscle innervation pattern of the levator auris longus (LAL) muscle from a SMA mouse (*Smn*$^{-/-}$*;SMN2*) [29]. The red line indicates the demarcation point between the rostral band of the muscle (to the right) and the caudal band (to the left). The left panel shows an example of a high-power confocal micrograph of neuromuscular junctions in the caudal band of the muscle at post-natal day 5 (green; immunohistochemically labelled 150kDa neurofilament and SV2 synaptic vesicle proteins to highlight the motor neuron / red; acetylcholine receptors on skeletal muscle fibres labelled with TRITC-conjugated alpha-bungarotoxin). Note the presence of widespread neuronal pathology evidenced by the loss of neuronal inputs to motor endplates and presence of neurofilament accumulations [29]. The right panel shows an example of a high-power confocal micrograph of neuromuscular junctions in the rostral band of the muscle at post-natal day 5. Note the preservation of motor neuron inputs, even at this late-symptomatic age. (B) A representative confocal micrograph showing immunohistochemically labelled neuromuscular junctions from the rostral band of the LAL from a SMA mouse at P1. Note the complete absence of any overt neuronal pathology (e.g. vacant endplates or neurofilament accumulations). (C) Bar chart (mean ± S.E.M.) showing muscle fibre diameter in the rostral band of the LAL from both SMA mice (*Smn*$^{-/-}$*;SMN2*) and littermate controls (*Smn*$^{+/+}$*;SMN2*) at P1. There was no denervation induced muscle fibre atrophy in the SMA mice ($P>0.05$; unpaired, two-tailed t test; $N>3$ mice per genotype). (D) Representative western blot showing reduced expression levels of SMN protein in the rostral band of the LAL from SMA mice

compared to littermate controls. Beta-V-Tubulin was used as a loading control. Scale bars = 20μm.

Figure 2. Increased levels of cell death in the rostral LAL from SMA mice. (A/B) Representative fluorescence micrographs of rostral LAL muscle preparations from an *Smn*$^{-/-}$*;SMN2* mouse (B) and a littermate control (A) immunohistochemically labelled for the cell death marker H2AX (green). Nuclei were labelled with TOPRO-3 (red). Almost all muscle nuclei in muscles from littermate control mice showed no, or weak, labelling (A), whereas strong H2Ax labelling was easily identified in SMA muscles (B). Images in panels A and B were taken with identical settings on the confocal microscope (e.g. laser intensity, gain, zoom, z-stack depth etc). (C) Bar chart (mean±s.e.m) showing a significant increase in the numbers of cells with intense H2AX labelling in the rostral LAL of *Smn*$^{-/-}$*;SMN2* mice (SMA) compared to littermate controls (Control) ($P<0.05$, Unpaired two-tailed t-test, N=3 muscles). Scale bar = 10μm.

Figure 3. Molecular pathology of SMA skeletal muscle is molecularly distinct from changes elicited following chronic or acute denervation. (A) Comparison of expression profiles of individual proteins identified in SMA muscle with expression changes observed in chronically denervated rodent muscle. Note that the molecular profile of SMA muscle was distinct from that in denervated muscle. NC = no change, NR = not reported, UP = increased expression, DOWN = decreased expression. (B) Bar chart (mean±s.e.m) showing expression levels of Vdac2 and parvalbumin in mouse *flexor digitorum brevis* muscles before (control) or 24 hours after (denervated) tibial nerve lesion. Neither protein showed a significant change in expression in denervated muscle ($P>0.05$; unpaired, two-tailed t test; N>3 mice per genotype).

Figure 4. Molecular modifications are also present in skeletal muscle from human SMA patients. (A) Representative fluorescent western blots on *quadriceps femoris* biopsy samples

from SMA patients (type II or type III; aged between 3 and 25 years old) and non-SMA controls showing levels of SMN protein, beta-V-tubulin (loading control), Vdac2 and parvalbumin. (B-D) Bar charts showing expression levels of SMN, Vdac2 and parvalbumin in human SMA patient muscle compared to controls. Data is shown for individual patients (black and white bars to the left of the hashed line) as well as mean±s.e.m for each genotype (right of the line). SMN levels were significantly decreased in SMA patients (*P<0.05; unpaired, two-tailed t test; panel B), Vdac2 levels were significantly increased (*P<0.05; unpaired, two-tailed t test; panel C) and parvalbumin levels were significantly decreased (*P<0.05; panel B).

Figure 5. Reversal of SMA-induced molecular pathology of skeletal muscle by treatment with SAHA. (A) Representative fluorescent western blots on *gastrocnemius* muscles from Taiwanese-SMA mice (SMA), littermate controls (Control) and SAHA-treated Taiwanese-SMA mice (SMA+SAHA) at P10 showing levels of SMN protein, beta-V-tubulin (loading control), Vdac2, parvalbumin and H2AX. (B-E) Bar charts (mean±s.e.m) showing expression levels of SMN, Vdac2, parvalbumin and H2AX. SMN levels were significantly decreased in Taiwanese-SMA mice compared to controls (***P<0.001; ANOVA with Tukey's post hoc test; panel B) and were significantly increased in SMA mice treated with SAHA (*P<0.05; panel B). Vdac2 levels were significantly increased in SMA mice (*P<0.05; panel C) and decreased by SAHA treatment (**P<0.01; panel C), returning to levels observed in littermate controls. Parvalbumin levels were significantly decreased in SMA mice (***P<0.001; panel D) but were increased by SAHA treatment (**P<0.01; panel D), restoring them to ~75% of those found in healthy control muscle. H2AX levels were significantly increased in SMA mice (***P<0.001; panel E) but were decreased by SAHA treatment (***P<0.001; panel E), restoring them to those found in healthy control muscle. n=19 independent measurements from N=5 mice (Control), n=17, N=5 (SMA), n=11, N=4 (SMA+SAHA).

Fig. 1

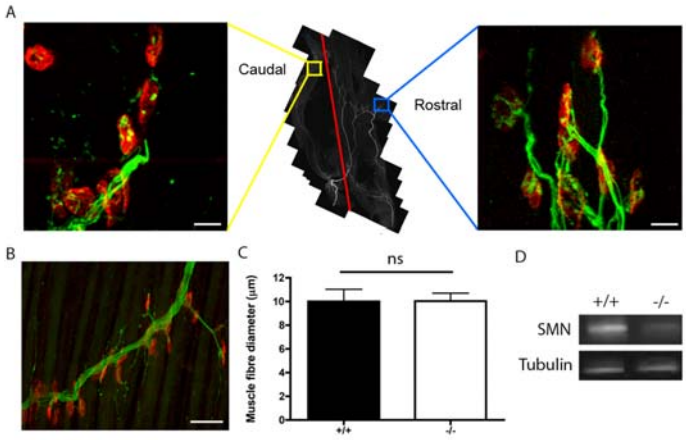

Fig. 2

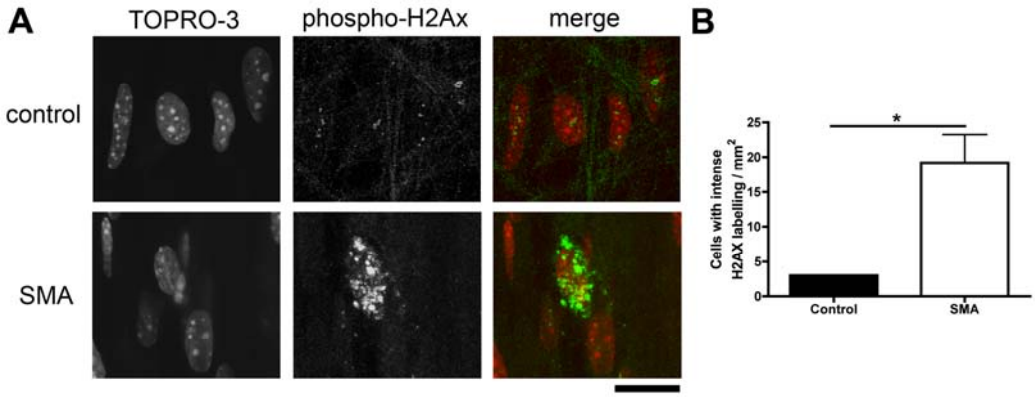

Fig. 3

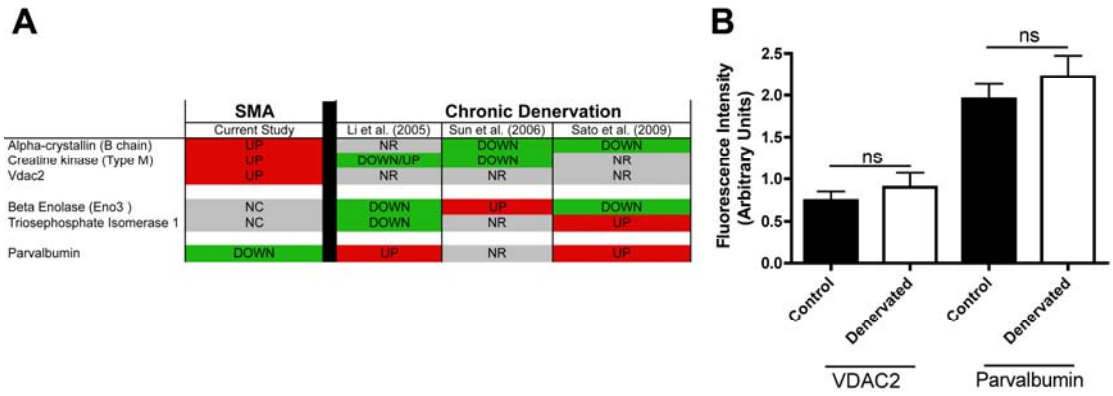

Fig. 4

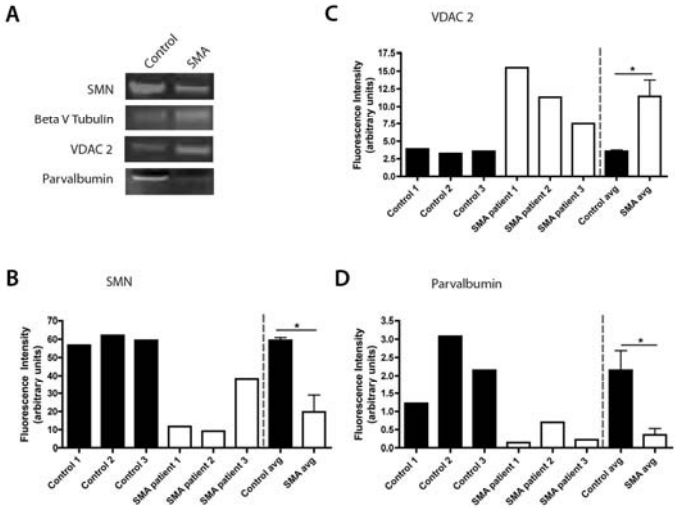

Fig. 5

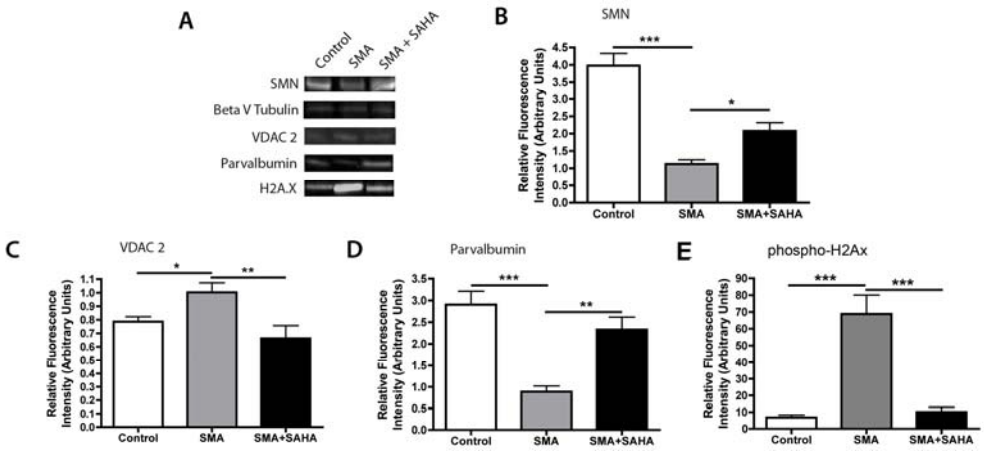

TABLES

Table I. Proteins upregulated >2 fold with peptide count >1 in the rostral band of LAL from SMA mice compared to littermate controls at P1

Gene name	Protein name	Accession number	Fold	Peptides	Score	Anova (p)
Vdac2	Voltage-dependent anion-selective channel protein 2	IPI00122547.1	5.12	2	113.23	4.05E-04
Rpl32 60S	Ribosomal protein L32	IPI00230623.8	3.33	2	77.74	5.92E-03
Actc1	Actin, alpha cardiac muscle	IPI00654242.1	3.07	6	420.13	1.52E-06
Acta1	Actin, alpha skeletal muscle	IPI00110827.1	3.01	6	447.06	1.61E-06
Atp5c1	ATP synthase subunit gamma	IPI00313475.1	2.95	2	116.8	1.59E-04
- 11 kDa protein	N/A	IPI00329998.3	2.58	2	117.08	4.67E-06
Alb	Serum albumin	IPI00131695.3	2.51	13	615.81	1.07E-05
Mylpf	Myosin regulatory light chain 2, skeletal muscle isoform	IPI00224549.3	2.5	6	372.77	5.08E-04
Rpl8 60S	Ribosomal protein L8	IPI00137787.3	2.48	2	92.06	9.31E-05
Pgk1	Phosphoglycerate kinase 1	IPI00555069.3	2.36	5	326.18	9.71E-08
Atp5b	ATP synthase subunit beta	IPI00468481.2	2.35	3	271.15	3.17E-05
Dcn	Decorin	IPI00123196.1	2.33	2	50.99	1.41E-04
Apoa1	Apolipoprotein A-I	IPI00121209.1	2.24	2	93.53	2.01E-04
Lgals1	Galectin-1	IPI00229517.5	2.23	3	174.29	5.17E-04
Mdh2	Malate dehydrogenase, mitochondrial	IPI00323592.2	2.21	3	143.52	6.59E-06
Cs	Citrate synthase	IPI00113141.1	2.17	2	85.12	3.66E-05
Atp5o	ATP synthase, H+ transporting, mitochondrial F1 complex, O subunit	IPI00118986.1	2.08	2	85.41	5.84E-04
Aco2	Aconitate hydratase	IPI00116074.1	2.05	5	219.6	9.84E-06
Trf	Serotransferrin	IPI00139788.2	2.02	11	645.3	9.07E-05
Afp	Alpha-fetoprotein	IPI00113163.1	2	5	288.77	1.20E-04

Table II. Proteins downregulated >2 fold with peptide count >1 in the rostral band of LAL from SMA mice compared to littermate controls at P1

Gene name	Protein name	Accession number	Fold	Peptides	Score	Anova (p)
P4hb	Prolyl 4-hydroxylase, beta polypeptide	IPI00122815.3	-2.66	3	111.53	6.29E-05
Pvalb	Parvalbumin alpha	IPI00230766.4	-2.65	2	90.44	3.72E-05
Rcn3	Reticulocalbin-3	IPI00221798.1	-2.28	2	173.67	1.35E-05
Rps7 40S	Ribosomal protein S7	IPI00136984.1	-2.15	2	63.7	4.38E-04
Anxa5	Annexin A5	IPI00317309.5	-2.05	2	98.22	8.74E-03
Hist1h1d	Histone H1.3	IPI00331597.6	-2.03	4	168.92	0.03

Table III. Systems level analysis of functional pathway changes in the rostral band of LAL muscle in SMA mice at P1

Function Annotation	Number of proteins	Percentage of candidate list	P-value	Proteins
skeletal and muscular disorder	44	53.0	2.31E-08	ACTA1, ACTB, ACTN2, ALB, ANXA2, ANXA5, APOA1, ATP5C1, BIN1, CA3, CASQ2, CKAP4, CLTC, CRYAB, DES, EEF2, EEF1G, FH, FHL1, FLNA, GPI, HNRNPA1, HNRNPA3, HSP90B1, HSPA8, HSPB1, LGALS1, MDH1, MYH8, MYL1, MYOM1, MYOM2, NONO, PDIA3, PFKM, PGK1, PKM2, PPIA, PVALB, RPL3, RPL32, TNNC2, TPM2, VIM
tumorigenesis	41	49.4	5.12E-06	ACTB, ACTC1, AFP, ALB, ANXA2, ANXA5, APOA1, ATP5C1, CA3, CKM, CRYAB, CSRP3, DCN, EIF4A1, FH, FLNA, FSCN1, GPI, HBB, HBD, HNRNPA1, HNRNPK, HSP90B1, HSPA8, HSPB1, LGALS1, MDH1, MYH8, MYLPF, P4HB, PA2G4, PGK1, PKM2, PPIA, SPTBN1, TNNC2, TPM1, TPM2, VDAC2, VIM, YWHAG
cell death	29	34.9	9.60E-04	ACTB, ACTC1, AFP, ALB, APOA1, BIN1, CCT7, CCT8, CRYAB, DCN, FLNA, GPI, HIST1H1C, HNRNPA1, HSPA8, HSPB1, LGALS1, MDH1, NME2, P4HB, PA2G4, PDIA3, PKM2, PPIA, PPID, TF, TPM1, VCL, VDAC2
inflammatory disorder	29	34.9	2.32E-02	ACO2, ACTA1, ACTB, ALB, ANXA5, APOA1, CA3, CLTC, CRYAB, EEF2, EEF1G, GPI, HBD, HNRNPA1, HNRNPA3, HNRNPK, HSP90B1, HSPA8, LGALS1, NONO, P4HB, PDIA3, PGK1, PPID, RPL32, TF, TPM2, VDAC2, VIM
growth of cells	24	28.9	1.18E-04	ACTB, AKR1B1, ALB, ANXA2, ATP5B, BIN1, CA3, CCT7, CRYAB, DCN, DES, EIF4A1, HNRNPA1, HNRNPK, LGALS1, NME2, PA2G4, PDIA3, PGK1, PKM2, SERPINH1, TF, TPM1, TPM2
cardiovascular disorder	24	28.9	2.01E-02	ACTA1, ACTC1, ACTN2, ALB, ANXA2, ANXA5, APOA1, BIN1, CA3, CASQ2, CKAP4, CKM, CRYAB, CS, CSRP3, DES, FHL1, GPI, MYH8, PPIA, SPTBN1, TPM1, VCL, VIM
proliferation of cells	23	27.7	1.10E-02	AFP, AKR1B1, ANXA2, APOA1, BIN1, CLTC, CRYAB, DCN, FHL1, FSCN1, GPI, HNRNPK, HSP90B1, LGALS1, NME2, PA2G4, PGK1, PPIA, SPTAN1, SPTBN1, TF, VIM, YWHAG
connective tissue disorder	21	25.3	1.38E-02	ACTA1, ALB, ANXA5, APOA1, CLTC, CRYAB, EEF2, EEF1G, FLNA, GPI, HNRNPA1, HNRNPA3, HSP90B1, HSPA8, LGALS1, NONO, PDIA3, PGK1, RPL32, TPM2, VIM
developmental disorder	15	18.1	9.47E-04	ACTC1, ALB, APOA1, CA3, CASQ2, CRYAB, CSRP3, DES, FLNA, HBB, MYOM1, SEC23A, TF, TPM1, VCL
progressive motor neuropathy	15	18.1	8.09E-03	ACTB, ANXA2, ANXA5, CA3, CRYAB, FH, HSPB1, MDH1, MYOM1, PDIA3, PDLIM5, PGK1, PVALB, RPL3, VIM
contraction of muscle	14	16.9	6.26E-12	ACTA1, ACTC1, ACTN2, ANXA6, CASQ2, CRYAB, DES, MYL1, MYLPF, MYOM1, MYOM2, TNNC2, TPM1, TPM2
cell movement	13	15.7	5.28E-03	ACTB, ANXA2, APOA1, FLNA, FSCN1, GPI, HSPB1, LGALS1, PA2G4, PPIA, TPM1, VCL, VIM
formation of filaments	10	12.0	1.07E-05	ACTA1, ACTC1, DES, FHL1, GPI, MYOM1, SERPINH1, TPM1, TPM2, VIM
metabolic process of carbohydrate	10	12.0	2.40E-04	AKR1B1, APOA1, CKM, CRYAB, CS, GPI, PFKM, PGK1, PKM2, PYGM
modification of protein	10	12.0	2.73E-02	APOA1, CCT7, CRYAB, HSPA8, LGALS1, P4HB, PDIA3, PPIA, PPID, SPTBN1
developmental process of muscle	9	10.8	5.75E-05	ACTC1, CRYAB, CSRP3, DES, HSP90B1, MYLPF, PKM2, TPM1, VCL
metabolism of protein	9	10.8	1.78E-02	EEF2, EIF4A1, FLNA, HNRNPK, HSPB1, RPL3, RPL6, RPL8, RPL32
binding of normal cells	7	8.4	2.97E-03	ANXA2, ANXA5, APOA1, CKAP4, DCN, PDIA3, VCL
myopathy	6	7.2	3.73E-05	ACTA1, BIN1, CRYAB, DES, FHL1, TPM2
proliferation of connective tissue cells	6	7.2	6.64E-03	DCN, GPI, LGALS1, PA2G4, PGK1, TF
modification of mRNA	5	6.0	1.38E-03	ALB, EIF4A1, HBB, HNRNPA1, NONO
development of cytoskeleton	5	6.0	2.66E-03	ACTB, DES, FLNA, FSCN1, TPM1
degradation of DNA	5	6.0	4.05E-03	ALB, BIN1, CRYAB, HNRNPA1, HSPB1
phosphorylation of protein	5	6.0	3.13E-02	APOA1, LGALS1, PDIA3, PPIA, SPTBN1

ABBREVIATIONS

FDB – Flexor digitorum brevis

HDACi – Histone deacetylase inhibitor

LAL – Levator auris longus

SAHA - Suberoylanilide hydroxamic acid

SMA – Spinal muscular atrophy

SMN – Survival motor neuron

VDAC2 - Voltage-dependent anion-selective channel protein 2